ISSN 1674-1056
http://cpb.iphy.ac.cn
http://iopscience.iop.org/cpb
中国物理 B
Chinese Physics
中国物理
Chinese Physics B

High mobility ultrathin ZnO p-n homojunction modulated by $Zn_{0.85}Mg_{0.15}O$ quantum barriers

Jing-Jing Yang(杨景景), Qing-Qing Fang(方庆清), Wen-Han Du(杜文汉), Ke-Ke Zhang, Da-Shun Dong(董大舜)
Citation: Chin. Phys. B . 2018, 27(3): 037804. **doi:** 10.1088/1674-1056/27/3/037804

Journal homepage: http://cpb.iphy.ac.cn; http://iopscience.iop.org/cpb

What follows is a list of articles you may be interested in

Raman spectrum study of δ -doped GaAs/AlAs multiple-quantum wells

Wei-Min Zheng(郑卫民), Wei-Yan Cong(丛伟艳), Su-Mei Li(李素梅), Ai-Fang Wang(王爱芳), Bin Li(李斌), Hai-Bei Huang(黄海北)
Chin. Phys. B . 2018, 27(1): 017302. **doi:** 10.1088/1674-1056/27/1/017302

Improvement of green InGaN-based LEDs efficiency using a novel quantum well structure

Yangfeng Li(李阳锋), Yang Jiang(江洋), Junhui Die(迭俊珲), Caiwei Wang(王彩玮), Shen Yan(严珅), Ziguang Ma(马紫光), Haiyan Wu(吴海燕), Lu Wang(王禄), Haiqiang Jia(贾海强), Wenxin Wang(王文新), Hong Chen(陈弘)
Chin. Phys. B . 2017, 26(8): 087311. **doi:** 10.1088/1674-1056/26/8/087311

Pure blue and white light electroluminescence in a multilayer organic light-emitting diode using a new blue emitter

Wei Na, Guo Kun-Ping, Zhou Peng-Chao, Yu Jian-Ning, Wei Bin, Zhang Jian-Hua
Chin. Phys. B . 2014, 23(7): 077802. **doi:** 10.1088/1674-1056/23/7/077802

Tandem white organic light-emitting diodes adopting a C_{60}: rubrene charge generation layer

Bi Wen-Tao, Wu Xiao-Ming, Hua Yu-Lin, Sun Jin-E, Xiao Zhi-Hui, Wang Li, Yin Shou-Gen
Chin. Phys. B . 2014, 23(1): 017803. **doi:** 10.1088/1674-1056/23/1/017803

Spin–orbit coupling effects on the in-plane optical anisotropy of semiconductor quantum wells

Yu Jin-Ling, Chen Yong-Hai, Lai Yun-Feng, Cheng Shu-Ying
Chin. Phys. B . 2014, 23(1): 017806. **doi:** 10.1088/1674-1056/23/1/017806

High mobility ultrathin ZnO p–n homojunction modulated by $Zn_{0.85}Mg_{0.15}O$ quantum barriers*

Jing-Jing Yang(杨景景)[1,2], Qing-Qing Fang(方庆清)[1,†], Wen-Han Du(杜文汉)[2,3,‡], Ke-Ke Zhang[3], and Da-Shun Dong(董大舜)[1]

[1] School of Physics and Materials Science, Anhui University, Hefei 230601, China
[2] Changzhou Institute of Technology, Changzhou 213002, China
[3] School of Materials Science and Engineering, Nanyang Technological University, Singapore

(Received 15 October 2017; revised manuscript received 22 December 2017; published online 11 February 2018)

The adding of ZnMgO asymmetric double barriers (ADB) in p-ZnO: (Li, N)/n-ZnO homojunction affects the p–n junction device performance prominently. Two different homojunctions are fabricated on Si (100) substrates by pulsed laser deposition; one is the traditional p-ZnO: (Li, N)/n-ZnO homojunction with different thicknesses named as S_1 (250 nm) and S_2 (500 nm), the other is the one with ADB embedded in the n-layer named as Q (265 nm). From the photoluminescence spectra, defect luminescence present in the S-series devices is effectively limited in the Q device. The current–voltage curve of the Q device shows Zener-diode rectification property because the two-dimensional electron gas tunnels through the narrow ZnMgO barrier under a reverse bias, thus decreasing the working p–n homojunction thickness from 500 nm to 265 nm. The ADB-modified homojunction shows higher carrier mobility in the Q device. The electroluminescence of the ZnO homojunction is improved in Q compared to S_2, because the holes in p-type ZnO (Li, N) can cross the wide ZnMgO barrier under a forward bias voltage into the ZnO quantum well. Therefore, electron–hole recombination occurs in the narrow bandgap of n-type ZnO, creating an ultraviolet light-emitting diode using the ZnO homojunction.

Keywords: ZnO p–n homojunction, light-emitting diodes, ZnMgO asymmetric double barriers

PACS: 78.67.De, 73.21.Fg, 68.35.Bg, 81.15.Fg **DOI:** 10.1088/1674-1056/27/3/037804

1. Introduction

ZnO is a wide band gap transparent II–VI semiconductor. It may be highly significant in future device applications.[1–8] Great efforts have been devoted to creating light-emitting diodes[9] and laser diodes[10–12] using ZnO. Band-gap engineering is used to create heterojunctions and quantum well structures (QWS) with matching material properties.[13] However, developing electrically pumped ZnO p–n junction devices is difficult because of the lack of reliable and controllable p-type ZnO.[14] Appropriate rectifying characteristics can be successfully achieved when the ZnO p–n junction thickness approaches micrometer-scale.[15] The transparent nature of ZnO p–n junctions permits their application in solar cell devices.[16] If the device thickness can be reduced, the transmittance in the wavelength range of the visible spectrum may be improved,[17] and applications using flexible substrates could be facilitated.[17–19] Therefore, maintaining device performance while reducing device thickness is an important development direction.

Previously, we have reported antimony (Li, N)-doped p-type ZnO[20] prepared by pulsed laser deposition. In this work, ZnO/ZnMgO asymmetric double barriers (ADB) are embedded to improve the performance of the ZnO p–n homojunction. Two different types of p-type/n-type ZnO homojunctions are prepared by pulsed laser deposition (PLD) on Si substrates. The ZnO p–n homojunctions use ZnO: (Li, N) and pure ZnO as the p- and n-layers, respectively; meanwhile, the Q ZnO p–n homojunctions have ZnO/ZnMgO ADB embedded in the n-type ZnO layer.

2. Material and methods

ADB structures in ZnO p–n homojunction were fabricated on Si substrates by pulse laser deposition. In order to determine whether the ADB functions well or not in the ZnO homojunction at RT, the ZnO/$Zn_{0.85}Mg_{0.15}O$ ADB, S-series p-ZnO: (Li, N)/n-ZnO homojunction, and Q p-ZnO: (Li, N) /ADB /n-ZnO homojunction were prepared by PLD separately.

The ZnO/$Zn_{0.85}Mg_{0.15}O$ ADB was deposited on Si(100) substrates, while the other ZnO homojunctions were deposited on Si(100) substrates using a KrF excimer laser ($\lambda = 248$ nm, full width at half-maximum FWHM = 30 ns). The energy of the laser was 190 mJ/pulse, and the pulse frequency was 4 Hz. ZnO, $Zn_{0.9}Li_{0.1}O$, and $Zn_{0.85}Mg_{0.15}O$ targets were syn-

*Project supported by the National Natural Science Foundation of China (Grant Nos. 61540071 and 11705016), Project of Natural Science Research of Higher Education in Jiangsu Province, China (Grant Nos. 17KJB510001 and 17KJB140002), Changzhou Sci&Tech Program, China (Grant No. CJ20160026), and Changzhou Institute of Technology Science Foundation, China (Grant No. YN1408).

†Corresponding author. E-mail: physfangqq@126.com
‡Corresponding author. E-mail: duwenhan@ntu.edu.sg

© 2018 Chinese Physical Society and IOP Publishing Ltd

thesized from high-purity ZnO, MgO, and Li_2O (99.999%) powders, which were ceramic-pressed and sintered at 1050 °C for 12 h in flowing air. The doping N_2 pressure was 2.3 Pa, and the growth temperature was 450 °C. The structure of $ZnO/Zn_{0.85}Mg_{0.15}O$ ADB is shown in Fig. 1, while the S and Q samples are shown in Fig. 2. Because the charge carrier in the ZnMgO layer is electrons,[14] we constructed QWSs of ZnO/ZnMgO/ZnO in the n-type layer. The electrodes were formed from a Ag (99.999%) target. The x-ray diffraction (XRD) data of the samples were obtained by a PHILIPS X'Pert PRO diffractometer, the absorption spectra were measured by a Hitachi U-4100 spectrophotometer, and the photoluminescence spectra were collected by a LABRAM-HR Raman spectrometer with a 325-nm laser light source. All measurements were performed at RT.

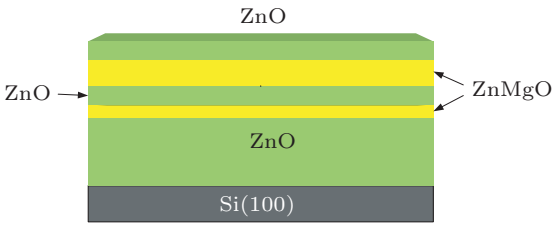


Fig. 1. (color online) Geometric structure of $ZnO/Zn_{0.85}Mg_{0.15}O$ ADB.

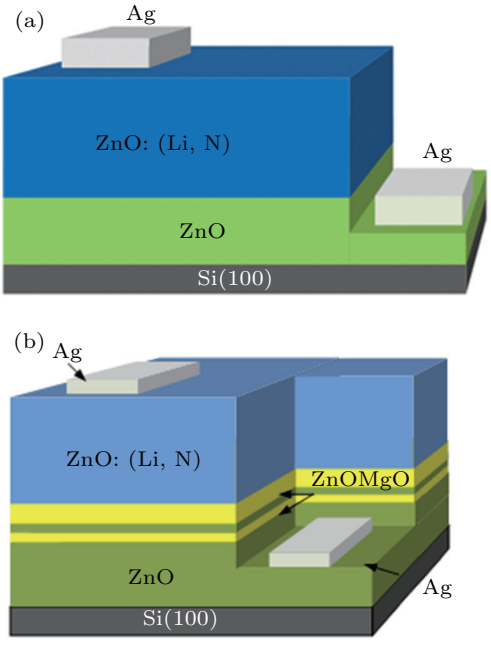


Fig. 2. (color online) Geometric structures of ZnO p–n junctions with or without ZnMgO ADB: (a) S-series p–n junctions without ZnMgO ADB; (b) Q p–n junctions with ZnMgO ADB.

As shown in Fig. 2(b), the $ZnO/Zn_{1-x}Mg_xO$ ADB is designed with the ADB structure consisting of two QWSs with different widths, forming the wide barrier (WB) and the narrow barrier (NB) and separated by a thin layer of ZnO. Thickness information of all samples is listed in Table 1 and Table 2.

Table 1. Thickness information of $ZnO/Zn_{0.85}Mg_{0.15}O$ ADB.

Sample	Film thicknesses of ZnO/ ZnMgO/ ZnO/ ZnMgO/ ZnO
$ZnO/Zn_{0.85}Mg_{0.15}O$ ADB	80 nm/ 3 nm/ 5 nm/ 7 nm/ 5 nm

Table 2. Thickness information of different ZnO p–n homojunctions.

Sample	p–n junction without ADB: ZnO: (Li,N)/ ZnO	p–n junctions with ADB: ZnO: (Li,N)/ ZnMgO/ ZnO/ ZnMgO/ ZnO
S_1	150 nm/ 100 nm	
S_2	300 nm/ 200 nm	
Q		150 nm/ 7 nm/ 5 nm/ 3 nm/ 100 nm

3. Results and discussion

3.1. Structure measurements

Figure 3 shows the XRD pattern of $ZnO/Zn_{0.85}Mg_{0.15}O$ ADB. An FWHM of ~0.24° for the ZnMgO(002) crystalline plane is shown. This demonstrates that $ZnO/Zn_{0.85}Mg_{0.15}O$ ADB has preferential orientation growth on Si substrate. Further distinguishing features in Fig. 3 include the ZnMgO (002) shoulder marked 1 in the pattern, similar to the monocrystalline Si (400) substrate peak marked 1′ in the inset. These similarities confirm the good crystalline property of the ZnMgO thin film.[21] Figure 4 presents a cross-section SEM image of the $ZnO/Zn_{0.85}Mg_{0.15}O$ ADB. The ZnO and $Zn_{0.85}Mg_{0.15}O$ layers are clearly visible in the ADB structure. The ADB thickness is ~110 nm, according to that specified in our design. The SEM image verifies that the $ZnO/Zn_{0.85}Mg_{0.15}O$ ADB is successfully deposited by our method.

Next, we inserted the $ZnO/Zn_{0.85}Mg_{0.15}O$ ADB in S-series p-ZnO: (Li, N)/n-ZnO homojunction and tested the optical properties of the resulting Q-series p-ZnO: (Li, N)/ADB/n-ZnO homojunction to confirm the realization of quantum effects.

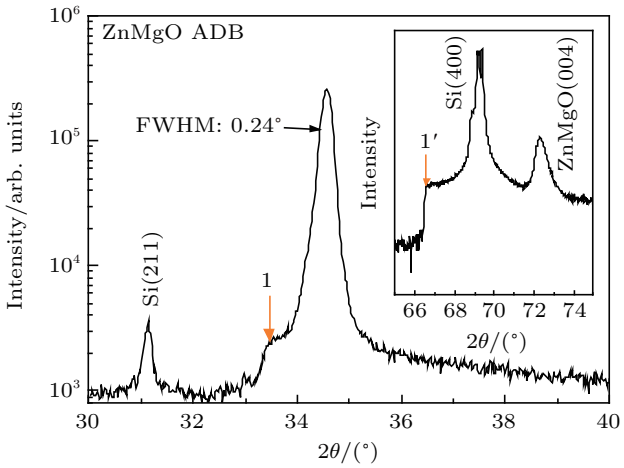


Fig. 3. (color online) XRD pattern of $ZnO/Zn_{0.85}Mg_{0.15}O$ ADB thin film on Si(100) substrate. Inset shows the XRD pattern at a different diffraction angle range of the same sample. The arrows marked with 1 and 1′ indicate the similarity of ZnMgO(002) and Si(400) XRD peak shapes.

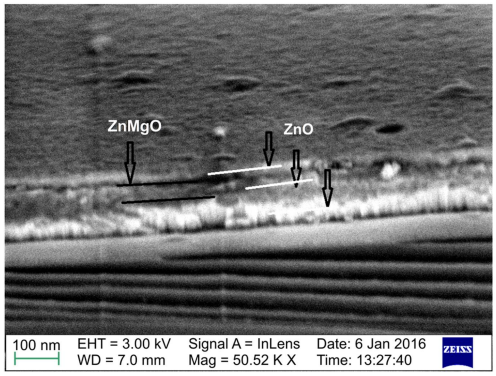


Fig. 4. (color online) Cross-section SEM image of ZnO/$Zn_{0.85}Mg_{0.15}O$ ADB thin film on silicon substrate.

3.2. Luminescence properties

In order to investigate the influence of the ADB on the performance of the homojunction, the photoluminescence spectra were obtained at RT using 325-nm laser light. Figure 5 shows the photoluminescence spectra of these devices. Comparing the spectra of samples Q and S, we find that the visible light peak (peak *B*) at 619 nm, which arises from the deep-energy-level defects in the S_1 and S_2 homojunctions, is effectively suppressed in the Q device. Considering the similarity in crystal quality between these two series, we infer that the decrease of peak *B* is caused by the adding of the ADB structure, which forms a barrier layer in the Q-series homojunction by creating a potential well. Luminescence peak *A* (centred at 381 nm), corresponding to the ZnO intrinsic photoluminescence is clearly strengthened in the Q device.[22] The exciton effect is improved in the 2-D system, thus enhancing the intrinsic transitions caused by free or localized excitons. This also indicates that the adding of ADB has a modulation effect in the Q: p-ZnO: (Li, N)/ADB/n-ZnO homojunction.

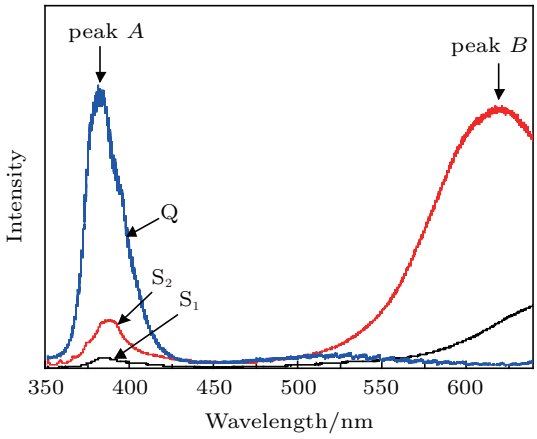


Fig. 5. (color online) Photoluminescence spectra of S_1, S_2, and Q.

3.3. Electrical properties

3.3.1. Current–voltage curve

In order to confirm the modulation by the added ADB structure, we tested the current–voltage (*I*–*V*) properties of all ZnO p–n homojunctions. All *I*–*V* measurements were performed using a Keithley 2611A source meter.

Figure 6 depicts the *I*–*V* curves of the samples deposited on Si (100). The inset demonstrates that the electrodes have good electrical contact. Two conclusions can be drawn from Fig. 6. First, all samples show obvious p–n junction rectifier features, excepting S_1, which forms an Ohmic contact. Second, the Q p–n homojunction obviously exhibits smaller V_{Bi} (0.92 V) than S_2, with an obvious Zener breakdown feature. S_1 forms an Ohmic contact because the p–n junction thickness is insufficient for a space-charge region. However, the Q device of nearly equal thickness shows typical *I*–*V* features of p–n junction rectifiers, implying that the ZnMgO ADB effectively promotes the p–n homojunction properties even in ultrathin layers of 265 nm.

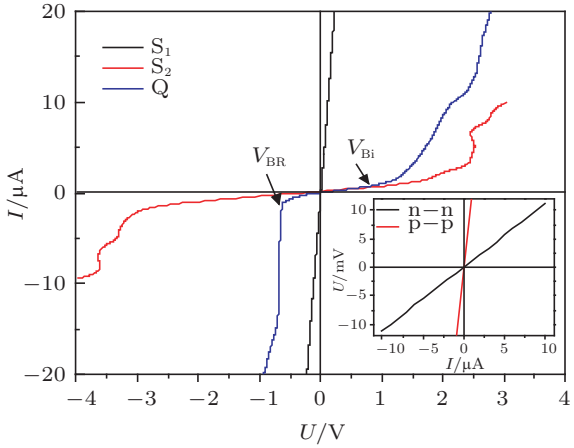


Fig. 6. (color online) *I*–*V* curves of ZnO p–n homojunctions with different conditions on Si substrates.

The Q device exhibits obvious Zener breakdown features while sample S_2 does not. It is known that, for $V_{BR} < 4E_g/e$, tunnelling occurs when the Q-series p–n homojunction operates under a reverse bias. Because the E_g of p-ZnO: (Li, N)/ADB/n-ZnO changes with the position in the energy band, we choose the lowest ZnO E_g of 3.36 eV for calculation. V_{BR} is 0.65 V, far less than the tunnelling upper limit of 13.4 V. At the ZnO/$Zn_{0.85}Mg_{0.15}O$ film interface, an internal field is formed by the total polarization between ZnO and $Zn_{0.85}Mg_{0.15}O$, including both spontaneous and piezoelectric polarizations.[23–25] Polarization-induced positive charges thereby form at the heterointerface, creating a 2-D electron gas (2DEG) confined in the ZnO QW. The energy band is inclined to equalize the energy level among different overlapping bands. Although the reverse bias voltage is very low, carriers in the ZnO wells can tunnel through the ZnMgO NB to the n-type conduction band. This field-induced inter-band tunnel effect causes electronic tunnelling transfer in the Q-series devices. Therefore, the ADB structure effectively shrinks the space-charge regions with thinner ZnO homojunction, confining the 2DEG to the ZnO active layer and thereby impelling

the 2DEG to pass through the band by the field-induced inter-band tunnelling effect under a small reverse bias.

3.3.2. Hall-effect

To determine how the ADB influences the electron mobility of the 2DEG, we performed Hall-effect measurements with electrodes shown in Fig. 7, and Ag electrodes placed at the four corners of the ADB structure. The active area of the sample is 1 cm^2. The Hall-effect measurements were conducted with an Accent HL5500PC system, with results listed in Table 3.

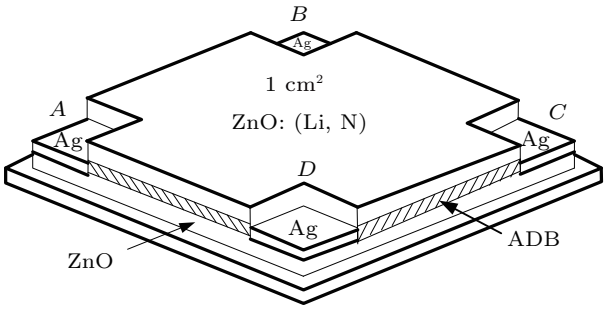


Fig. 7. The four-probe method used for Hall effect test.

Table 3. Electrical properties of ZnO: (Li, N)/ADB/ZnO thin films.

Thin films	Magnetic field/10^{-4} T	Resistivity /Ω·cm	Carrier density/cm^{-3}	Hall mobility μ/cm^2·V^{-1}·s^{-1}
S_1 (250 nm)	1000	0.24	1.95×10^{18}	1.3
S_2 (500 nm)	1000	1.62	1.78×10^{16}	2.16×10^{2}
Q (265 nm)	1000	4.20×10^{-2}	8.93×10^{16}	1.66×10^{3}
	1000	3.24×10^{-2}	3.47×10^{17}	5.53×10^{2}
	1000	2.78×10^{-2}	7.11×10^{17}	3.14×10^{2}
	1000	5.39×10^{-2}	3.48×10^{17}	3.32×10^{2}

The electrical properties were measured in the Q device under 0.1 T magnetic field to determine the carrier density and mobility. The Hall mobility μ in the Q device is much higher than that in the S-series devices, and the resistivity of the Q sample is reduced to 10^{-2} Ω·cm compared to 1.62 Ω·cm of the S_2 sample. In contrast to S_2, sample Q achieves a higher Hall mobility even at a thickness reduced by almost 50%. Clearly, in ZnO: (Li, N)/ADB/ZnO p–n junctions, the ADB structures cause device modulations. 2DEGs have increased mobility and electrons become concentrated in the active layers of ZnO QWSs.

3.4. Electroluminescence of ZnO: (Li, N)/ADB/ZnO p–n homojunction

Electroluminescence (EL) characterizations were performed to determine the luminescence properties of S_2 and Q p–n homojunctions. A monochromator (ARSSP2557) was used to collect the emission and EL spectra.

Figure 8 shows the EL spectra of the S_2 and Q devices operated with an injection current of 20 mA and a forward bias of 5 V. Sample S_2 shows almost no luminance; Q exhibits a quasi-equidistant pattern of luminescence peaks, similar to that reported for ZnO nano-wire/film p–n junctions.[26] The average spacing between modes $\Delta\lambda$ is 5.1 nm for the selected peaks denoted by arrows in Fig. 8. We propose that the ZnO/ZnMgO interface on both sides of the ZnO QWS operates as a Fabry–Perot (F–P) cavity[27] because the $\Delta\lambda$ coincides with the 5-nm width of the ZnO QWS. In the LED utilizing Q p–n homojunction, the forward bias causes the holes in p-type ZnO to pass through the barriers into the active layer of ZnO QWSs, instead of causing electron transfer through the ZnMgO WB. The homojunction with ZnMgO ADB has stronger exciton recombination efficiencies compared to the normal p–n homojunction. Therefore, the Q device exhibits UV-wavelength light-emitting characteristics. This demonstrates that the ZnMgO ADB embedded in ZnO homojunction obviously improves the EL characteristics and effectively reduces the device thickness.

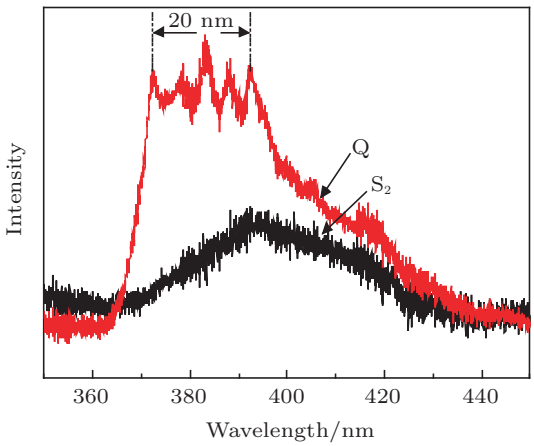


Fig. 8. (color online) Electroluminescence spectra of S_2 and Q ZnO homojunctions.

The carrier transport mechanism of the Q homojunction is shown schematically in Fig. 9. In the ZnO QWS, the energy band is inclined, equalizing the energy levels in different overlapping bands. Under very low reverse bias voltages, the carriers in the QWS will tunnel to the n-type ZnO through the NB. This field-induced inter-band tunnel effect causes carrier tunnelling transfer in the Q devices. The $Zn_{0.85}Mg_{0.15}O$ ADB also effectively concentrates electrons in the active layers of the ZnO QWSs. Importantly, under injection currents at the forward bias of 5 V, the holes in p-type ZnO pass through the ZnMgO WB barrier into the active-layer of the ZnO QWSs, enhancing exciton recombination in the wells. The homojunction with ZnMgO ADB shows higher exciton recombination efficiencies than the normal p–n homojunction. Therefore, the ZnMgO ADB improves the EL properties of the ZnO homojunction to display UV-wavelength light-emitting characteristics at RT.

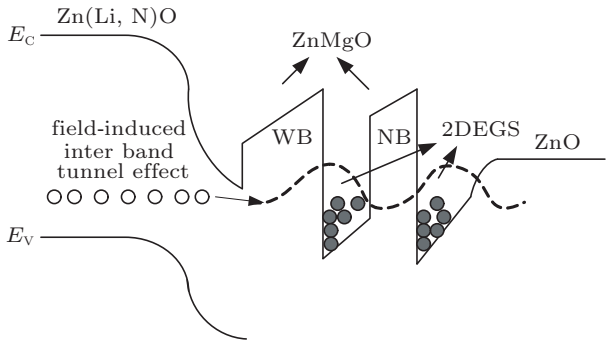


Fig. 9. The carrier transport schematic diagram of field-induced inter band tunnel effect of ADB-added ZnO p–n homojunction.

4. Conclusion

A $Zn_{0.85}Mg_{0.15}O$ ADB structure is added into the p-ZnO: (Li, N)/n-ZnO p–n homojunction to study the effects of the ADB on the junction performance. The $Zn_{0.85}Mg_{0.15}O$ ADB shows a modulation effect in the ZnO p–n homojunction at RT. For unmodified wide-band-gap semiconductors, such as ZnO, the electron tunnelling probability is very low, which greatly reduces the quantum efficiency. However, we find that the adding of $Zn_{0.85}Mg_{0.15}O$ ADB enhances the performance of the p–n homojunction in ultrathin films (265 nm) effectively, and a field-induced inter-band tunnelling effect in the ZnO: (Li, N)/ZnO p–n homojunction is observed under very small reverse bias voltages facilitated by the ADB design. Furthermore, the ZnO p–n homojunction with ZnMgO ADB has stronger exciton recombination efficiencies than the ZnO p–n homojunction without ZnMgO ADB, exhibiting UV-wavelength light-emitting characteristics at lower thicknesses and higher Hall mobility. This means that the adding of ZnMgO ADB structures in ZnO homojunction can greatly improve the performance of the ultrathin ZnO p–n homojunction. The device modification demonstrates increased performance in both rectifying characteristics and EL properties.

References

[1] Ding K, Ullah M B, Avrutina V, Özgür Ü and Morkoç H 2017 *Appl. Phys. Lett.* **111** 182101

[2] Toporkov M, Demchenko D O, Zolnai Z, Volk J, Avrutin V and Morkoc H 2016 *J. Appl. Phys.* **119** 095311

[3] Ullah M B, Avrutin V, Nakagawara T, Hafiz S, Altuntas I and Morkoc H 2017 *J. Appl. Phys.* **121** 185704

[4] Falson J, Kozuka Y, Uchida M, Smet J H, Arima T H, Tsukazaki A and Kawasaki M 2016 *Sci. Rep.* **6** 26598

[5] Ardaravičius L, Kiprijanovič O, Liberis J, Ramonas M, Šermukšnis E, Matulionis A, Toporkov M, Avrutin V, Özgür Ü and Morkoç H 2017 *Mater. Res. Express* **4** 066301

[6] Khan M A, Singh S, Mukherjee S and Kranti A 2017 *IEEE Trans. Electron Devices* **64** 1015

[7] Wang Z, He H P, Pan X H and Ye Z Z 2016 *Appl. Phys. A* **122** 962

[8] Xu C X, Chen W, Pan X H, Chen S S, Ye Z Z and Huang J Y 2016 *J. Cryst. Growth* **449** 92

[9] Przezdziecka E, Wierzbicka A, Reszka A, Goscinski K, Droba A and Jakiela R 2013 *J. Phys. D: Appl. Phys.* **46** 035101

[10] Chu S, Lim J H, Mandalapu L J, Yang Z, Li L and Liu J L 2008 *Appl. Phy. Lett.* **92** 152103

[11] Park T Y, Choi Y S, Kim S M, Jung G Y, Park S J and Kwon B J 2011 *Appl. Phys. Lett.* **98** 251111

[12] Zhang H Z, Shen R S, Liang H W, Liu Y D, Liu Y and Xia X C 2013 *J. Phys. D: Appl. Phys.* **46** 065101

[13] Su S C, Zhu H, Zhang L X, He M, Zhao L Z and Yu S F 2013 *Appl. Phys. Lett.* **103** 131104

[14] Park C H, Zhang S B and Wei S H 2002 *Phys. Rev. B* **66** 073202

[15] Xu W Z, Ye Z Z and Zeng Y J 2006 *Appl. Phys. Lett.* **88** 173506

[16] Koichi M, Ryota S, Tomoaki I, Daisuke Y, Hyunwoong S, Kazunori K, Masaharu S and Naho I 2015 *Thin Solid Films* **587** 106

[17] Hao X, Ma J, Zhang D, Yang T and Ma H 2002 *Appl. Surf. Sci.* **189** 137

[18] Yuan W, Zhu L P, Ye Z Z and Gu X Q 2009 *Appl. Surf. Sci.* **256** 1452

[19] Kim Y J, Lee H S, Noh J S, Kim Y J and Lee H S 2016 *Thin Solid Films* **603** 160

[20] Yang J J, Fang Q Q, Wang W N, Wang D D and Wang C 2014 *J. Appl. Phys.* **115** 124509

[21] Zha K L Chen G P, Juliana H Maria C and Shen A D 2015 *J. Cryst. Growth* **425** 221

[22] Chen W, Pan X H, Ye Z Z, Chen S S, Zhang H H, Ding P L and Huang B J 2015 *Appl. Phys. A* **119** 647

[23] Ye J D, Pannirselvam S, Lim S T, Bi J F, Sun X W, Lo G Q and Toe K L 2010 *Appl. Phys. Lett.* **97** 111908

[24] Zhang B P, Liu B L, Yu J Z, Wang Q M, Liu C Y and Liu Y C 2007 *Appl. Phys. Lett.* **90** 11213

[25] Stölzel M, Müller A, Benndorf G, Lorenz M, Patzig C and Höche T 2014 *Appl. Phys. Lett.* **104** 192102

[26] Chu S, Wang G P Zhou W H, Lin Y Q, Chernyak L Zhao J Z, Kong J Y, Li L, Ren J J and Liu J L 2011 *Nat. Nanotech.* **6** 175

[27] Welna M, Kudrawiec R, Misiewicz J, Yano M, Koike K and Sasa S 2015 *Phys. Status Solidi a* **211** 780